ELSEVIER

Nuclear Engineering and Design 156 (1995) 401–410

Nuclear Engineering and Design

Rupture and fragmentation of pressurized pipes and fast reactor fuel pins

I.J. Ford

Theoretical Studies Department, AEA Technology, 424.4, Harwell Laboratory, Didcot, Oxon. OX11 0RA, UK

Abstract

A model of axial crack propagation in a pressurized tube is developed which predicts the crack velocity and deformation geometry and the minimum driving pressure. Emphasis is placed upon the stability of propagation. The model also offers a criterion for the appearance of multiple cracks and subsequent fragmentation of the tube wall due to excessive axial bending strains. The model is applied to the rupture of gas pipelines, PWR coolant pipes and fast reactor fuel pins.

1. Introduction

Fast reactor safety studies often require consideration of the rupture of the fuel pins by a build-up of internal pressure, largely due to the melting of the fuel contained within the cladding tube. The subsequent ejection of fuel into the coolant channels and the later development of the accident are then affected by the mode of failure. The cross-sectional area of the hole produced in the cladding will determine the rate of fuel ejection and the axial extent of the opening will have an important bearing on subsequent axial fuel motion.

Although a rupture which remains localized presents the possibility of fuel concentration at the failure site, the opposite extreme, where a rip propagates large distances, "unzipping" the fuel pin, could lead to the coherent release of a large proportion of the fuel into the channels, which may lead to dangerous rates of energy release due to molten fuel–coolant interactions. Clearly it would be an advantage to be able to predict the extent of rupture propagation in a variety of conditions.

A model of the process has been developed (Ford, 1992a) based on mechanistic considerations of the energetics of a running crack in a cylindrical tube and on simple ideas concerning the depressurization of the pin. The model treats a single axial crack in the cladding, running in opposite directions away from the failure site, leaving the clad cross-section deformed into a U-shape. Energy sources (internal gas pressure, elastic relaxations) and dissipation mechanisms (material accelerations, plastic deformation and fracture work) are identified and evaluated, leading to an equation for the steady state crack velocity.

The model has recently been developed further (Ford, 1992b) based on circular deformed cross-sections and including a gas depressurization

Elsevier Science S.A.
SSDI 0029-5493(94)00963-5

model and a criterion for clad fragmentation. These developments will be described below. Section 2 considers the mechanics and geometry of a crack in steady state motion, leading to a partial determination of the clad deformation and an equation for the crack velocity. Section 3 describes experimental results for crack propagation in highly pressurized gas pipelines and introduces a model of gas decompression which determines the driving pressure to be inserted into the crack velocity equation. Experimental data are used to fix a remaining parameter of the model concerned with the crack tip length. Some calculations relevant to PWR steam pipes are given in Section 4, while in Section 5 the propagation of axial cracks in fuel pin cladding tubes is considered. Crack velocities are estimated and the likelihood of fragmentation rather than stable crack propagation is assessed. Some comparisons are made with experiments from the CABRI-1 programme of fuel pin rupture experiments (Cranga, 1990). The model is discussed in Section 6 and conclusions are given.

2. Crack mechanics and geometry

A description of crack geometry has been adopted based on the deformation observed in a series of tube rupture experiments (Buxton, unpublished). Cross-sections of the tubes were deformed into broken circles as illustrated in Fig. 1. The radial displacement $w(z)$ of the shell is taken to be

$$w(z)=\begin{cases}0, & z<0\\ \delta\sin^2\left(\dfrac{\pi z}{2a}\right), & 0<z<a\\ \delta & z>a\end{cases}$$

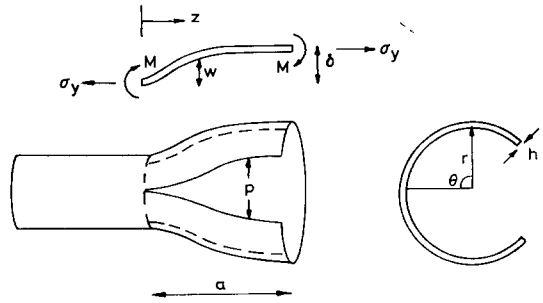

Fig. 1. Geometry of an axially propagating crack in a ruptured tube, with the paths of possible multiple cracks shown as broken lines.

where z is an axial coordinate measured from the crack tip, a is the length of the crack tip region within which the tube wall deformation occurs and δ is the maximum radial displacement. Assuming no circumferential straining, the crack opening is equal to $2\pi w(z)$.

The dimensions of the deformation, a and δ, are determined by a consideration of the equilibrium conditions of a steady state running crack. An axial element of the deforming region is shown in Fig. 1. An ideal rigid–perfectly plastic material is considered. The element is acted upon by the internal pressure, axial stresses in the tube wall and a cohesive stress acting at the crack tip. In addition, bending moments are introduced owing to the curvature at the ends. The precise determination of the system of forces and moments is difficult, however. To begin with, the exact distribution of internal pressure along the element is not known, though models have been proposed which suggest an exponentially decaying pressure profile when the tube is gas pressured. Secondly, the element is subjected to a combination of tension and bending, the precise mixture being determined by the location of the undeformed neutral axis along the element. Thirdly, azimuthal plastic bending complicates the stress analysis in the axial elements, with the consequence that axial stresses below the yield stress are sufficient for plastic yield. With all these complications present, the approach used here has been to use maximum stresses and moments and to investigate the resulting form of the mechanics equations. The terms will be altered in a more careful treatment only by numerical coefficients.

Accordingly, the axial tensile stress on the element is taken to be σ_y and the bending moment on each end is $M=\sigma_y h/4$, where σ_y is the yield stress and h is the wall thickness. The internal pressure is assumed to be a constant p throughout the deforming region. Equilibrium of moments about the crack tip then gives

$$\frac{pa^2}{2}=\frac{2\sigma_y h^2}{4}+\delta h\sigma_y \qquad (1)$$

which provides a link between the two unknown geometrical parameters a and δ. The complete

determination of the geometry requires another relationship specifying a or δ and this will be discussed in the next section.

In a steady state the energy sources, namely work done on the tube by the internal pressure plus elastic relaxation following fracture, should balance the energy dissipation, comprising fracture work, plastic work and kinetic losses. The work rate performed by the internal pressure is

$$\dot{W} = 2\pi \int_{-\pi}^{\pi} \int_{0}^{a} r \, \mathrm{d}z p \dot{w} \tag{2}$$

where r is the radius of the tube. Rates of change in energies are consistently replaced in the following by calculations of work done divided by a time scale a/v, where v is the crack velocity. Accordingly,

$$\dot{W} = \pi r \delta v p \tag{3}$$

Similarly, the elastic energy release rate $\dot{A}$ is

$$\dot{A} = \frac{\pi r h v \sigma_\theta^2}{E} \tag{4}$$

where σ_θ is the hoop stress ahead of the crack (equal to pr/h) and E is the Young's modulus.

The dissipative mechanism of fracture surface creation leads to a work rate

$$\dot{F} = \frac{K^2 h v}{E} \tag{5}$$

where K is the ductile fracture toughness characterizing the energy required to create new surface with associated local plastic deformation. The rate of plastic work can be considered as the sum of two components corresponding to bending in the azimuthal and axial directions. Azimuthal bending leads to a work rate

$$\dot{\Gamma}_{\mathrm{az}} = \frac{\pi}{4} \delta v \sigma_{\mathrm{y}} \frac{h^2}{r} \tag{6}$$

For axial bending, taking account of the subsequent unbending of the deformed section, the dissipation rate is

$$\dot{\Gamma}_{\mathrm{ax}} = \pi^2 \delta v \sigma_{\mathrm{y}} r \frac{h^2}{a^2} \tag{7}$$

Both calculations assume a rigid–perfectly plastic material and take no account of the biaxial stress conditions. The ratio of $\dot{\Gamma}_{\mathrm{ax}}$ to $\dot{\Gamma}_{\mathrm{az}}$ is $\pi(2r/a)^2$. Therefore plastic work is dominated by axial bending for short cracks (compared with the radius), while azimuthal bending is more important for long cracks. At this point the treatment of pipe rupture propagation by Freund and Parks (1980) should be mentioned. There it was explicitly assumed that the deforming region was four times the radius of the pipe and so $\dot{\Gamma}_{\mathrm{ax}}$ was ignored.

Finally, the kinetic energy dissipation rate can be calculated corresponding to the need to bring the tube wall into motion. This is

$$\dot{T} = \frac{\pi^2}{8} \rho_{\mathrm{c}} h r \delta^2 \frac{v^3}{a^2} \tag{8}$$

where ρ_{c} is the density of the tube material. By balancing energy sources and sinks at steady state, we have

$$\dot{T} + \dot{\Gamma}_{\mathrm{ax}} + \dot{\Gamma}_{\mathrm{az}} + \dot{F} = \dot{W} + \dot{A} \tag{9}$$

which leads to an equation for the crack velocity

$$v^2 = \frac{8a^2}{\rho_{\mathrm{c}} \delta h \pi^2} \left[p - \frac{\pi \sigma_{\mathrm{y}} h^2}{a^2} - \frac{\sigma_{\mathrm{y}} h^2}{4r^2} + \left(\sigma_\theta^2 - \frac{K^2}{\pi r} \right) \frac{h}{E\delta} \right] \tag{10}$$

if the right-hand side of this equation is positive and $v = 0$ otherwise.

The maximum bending strains in the tube wall are

$$\epsilon_z = \frac{\delta h \pi^2}{4a^2} \tag{11}$$

for axial bending and

$$\epsilon_\theta = \frac{\delta h}{2r^2} \tag{12}$$

for azimuthal bending. Comparing ϵ_z with the ductility, i.e. the fracture strain, now provides a criterion for fragmentation. This would be initiated by circumferential cracking from the tip of the axial crack, followed by the appearance of additional axial cracks, as illustrated in Fig. 1.

3. Gas pipeline rupture

To test the model described in Section 2, we use experimental data on the propagation of axial cracks in large diameter gas pipelines (Freund, 1980; Ives, 1974; Kanninen, 1976; Maxey, 1973). These studies were designed to improve safeguards against the propagation of a crack for large distances away from a gas pipeline failure site. The main differences between the gas pipe and the fuel pin cases are that (a) the dimensions are very different and (b) the pressurizing medium for the gas pipe studies was air or natural gas, whereas for the fuel pin the internal pressure can be provided by solid or molten fuel or possibly by fission gas alone. The behaviour can be greatly affected by the nature of the pressurizing medium, since it determines the loading profile (Ford, 1992c).

For the gas pipeline case a model of gas decompression is needed in order to relate the crack-driving pressure p to the initial pressure in the pipe, p_L. A one-dimensional gas dynamics treatment provides the pressure which is maintained at the tip of a crack running at velocity v (Kanninen, 1976; Liepmann, 1957). If the crack velocity is greater than the speed v_s of sound in the gas ($v_s = (\gamma kT/m)^{1/2}$, with k the Boltzmann constant, T the absolute temperature and m the molecular mass of the gas), then $p = p_L$, otherwise

$$p = p_L\left(\frac{2}{\gamma+1} + \frac{\gamma-1}{\gamma+1}\frac{v}{v_s}\right)^{2\gamma/(\gamma-1)} \tag{13}$$

where γ is the ratio of the specific heat of the gas at constant pressure to that at constant volume. This result is derived from a model where gas is allowed to escape from a semi-infinite duct, the end of which moves at a velocity v. With $\gamma \approx 1.4$ for air, Eq. (13) implies a minimum driving pressure of $0.28p_L$.

This model for gas decompression must be coupled to the crack velocity expression, Eq. (10), in order to produce a self-consistent steady state. This procedure is illustrated in Fig. 2, which represents conditions used in test A31(CA4) of the programme carried out by Maxey et al. (1973). The pipe was pressurized with natural gas with $\gamma = 1.3$ and $v_s = 396\ \mathrm{m\ s^{-1}}$. The v–p decompression curve is illustrated with $p_L = 7.92$ MPa, the initial pressure in the test. The yield stress was 484 MPa, $r = 46$ cm and $h = 0.84$ cm, so p_L was about 90% of the yield pressure $p_y = \sigma_y h/r$, which was 8.84 MPa. Assigning a value of K is rather uncertain, unfortunately. Standard pipeline steel (X60 grade) is asserted to have a toughness of 439 MPa $\mathrm{m}^{1/2}$ (Hahn, 1973). A procedure based on equating measured Charpy energies to K^2/E leads to a value of 335 MPa $\mathrm{m}^{1/2}$ (Freund, 1980). Fortunately, calculations seem not to depend strongly on the precise value (see Table 1) and the latter has been used. A set of velocity curves is shown in Fig. 2, derived from Eq. (10), over the full range of crack-driving pressures from 0 to p_y. The remaining geometrical uncertainty in the model, referred to earlier, is removed by the parametrization

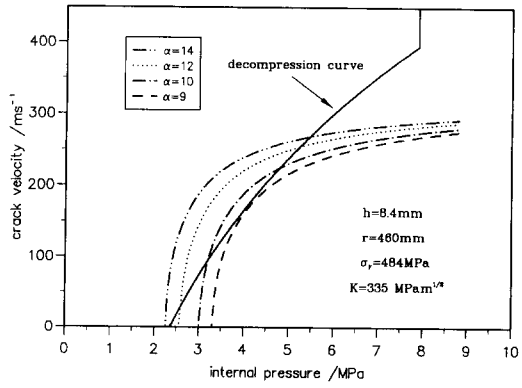

Fig. 2. Crack velocity against internal pressure in gas pipeline test A31(CA4). Also shown is the decompression pressure expected from gas dynamics.

$$a^2 = \alpha r h \tag{14}$$

where α is a constant. This form has been used in some other treatments (Maxey, 1973) with $\alpha = 9$, based upon the observed transition from propagating to arrested cracks as a function of pressure. The Young's modulus was taken to be 2×10^5 MPa and the steel density is 7770 kg m^{-3}.

Self-consistent steady propagation conditions occur where the crack velocity and decompression curves intersect. An additional requirement is that the decompression curve should have the greater slope at the intersection. This ensures that the

Table 1
Analysis of test of crack propagation in gas pipelines

Test	r (mm)	h (mm)	p_L (MPa)	σ_y (MPa)	K (MPa m$^{1/2}$)	v (m s^{-1}) (Model)	v (m s^{-1}) (experiment)	Comments
A31(CA4)	460	8.4	7.92	484	335 439	261 253	216–307	Natural gas (Freund, 1980; Maxey, 1973; Kanninen, 1976)
A32(CA5)	460	8.4	5.86	459	335	225	221–253	Natural gas (Maxey, 1973; Kanninen, 1976)
SF-12W	530	9.5	6.41	531	335	269	244	Air test (Ives, 1974; Freund, 1980)

situation is stable: if the crack ran faster, the driving pressure would increase according to the decompression curve, but this would take the tube into the net energy-dissipating region above the steady crack velocity curve shown. This would slow the crack and thus the system would return to equilibrium. The intersection at the higher pressure is therefore selected, the low pressure intersection being unstable.

Since the median experimental velocity was reported to be 260 m s^{-1} (with an uncertainty of about 20%), this constrains α to be in the range 12–14. This is checked in Fig. 3, which shows calculations made for test A32(CA5) (Kanninen, 1976; Maxey, 1973). The crack velocity for this test was reported to lie in the range 221–253 m s^{-1}. From these analyses, $\alpha = 14$ is selected as a reasonable fit. Results are equally encouraging for test SF-12W (Ives, 1974) which used air as the pressurizing medium, with $\gamma = 1.4$ and $v_s = 341$ m s^{-1}. Fig. 4 demonstrates that the intersection of the crack velocity curve and the decompression curve starting from an initial, experimental, pressure of 6.41 MPa lies reasonably close to the observed crack speed of 244 m s^{-1}. Also shown are decompression curves starting from 5 MPa and the yield pressure 9.52 MPa. Possible crack velocities clearly lie between about 300 and 200 m s^{-1} depending on p_L. Below a critical initial pressure the crack will not propagate in a stable fashion. This corresponds to the failure of the decompression curve and crack velocity curves to intersect. Equivalently, there is a minimum crack-driving pressure, in this case about 3.2 MPa or $0.37p_y$. This corresponds quite well to the arrest–propagate transition stress proposed by Maxey et al. (1973, 1974), which is approximately $0.3p_y$. The analysis of the tests is summarized in Table 1.

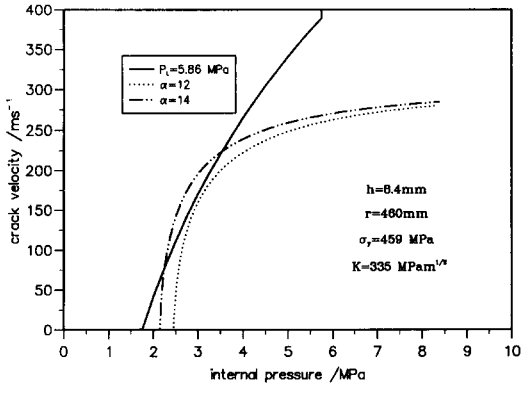

Fig. 3. Crack velocity against internal pressure in gas pipeline test A32(CA5). Also shown is the appropriate decompression curve.

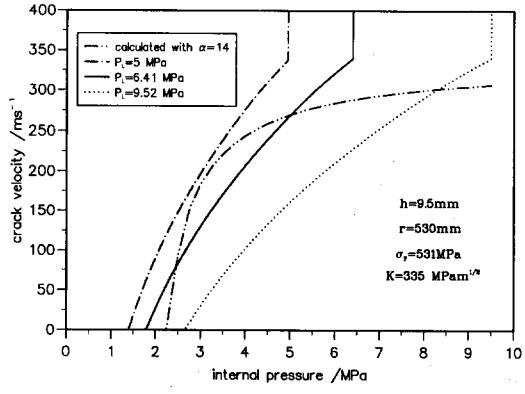

Fig. 4. Crack velocity against internal pressure for gas pipeline test SF-12W. Several gas decompression curves are shown for a range of initial conditions.

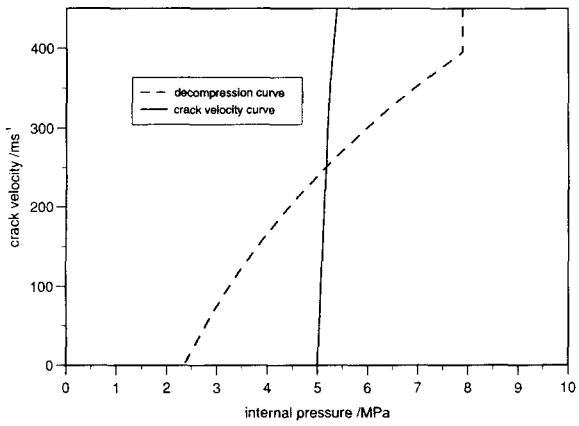

Fig. 5. Crack velocity prediction from Freund and Parks (1980) together with decompression curve for test A31(CA4), for comparison with Fig. 2.

It is useful at this stage to compare the present model with that of Freund and Parks (1980), who made a similar analysis of energy sources and sinks. The main geometrical difference compared with the present treatment is the inclusion of an unfractured membrane of material a distance R into the deforming crack tip region. The crack opening is given by the critical displacement (Brock, 1978). The geometry is determined by the choices $a = 4r$ and $R = 0.75r$, axial bending is ignored and the driving pressure is assumed to decay linearly between $z = 0$ and a. The resulting crack velocity curve for test A31(CA4) is shown in Fig. 5 (compare with Fig. 2). The decompression curve and crack velocity curve intersect at about the right velocity, but the equilibrium is unstable and will not be supported for long.

So far it has been assumed that the pipes are infinitely long such that there is sufficient gas within the pipe at distances far from the crack to maintain the driving pressure at the crack tip at a value which depends only on the crack velocity, given by Eq. (13). In reality the gas supply within the pipe is finite and eventually this will have an effect on the crack-driving pressure. The decompression curve in Fig. 2, for example, will move to the left as this effect becomes stronger: the driving pressure will fall for a given crack velocity. A model for this effect will depend on the particular details of the pipe geometry, but in general it can be seen that the equilibrium velocity will fall as the intersection between the decompression curve and the crack velocity curve moves to the left. Ultimately the two curves will fail to intersect, the system will then become energy dissipative and the crack arrests. The final deceleration will be rapid, owing to the shape of the curves, and crack arrest is abrupt.

Another mechanism of bringing about crack arrest is to insert sections along the pipe which have different deformation and fracture characteristics. For example, if the crack entered a region of pipe with a higher yield stress, the energy balance would be altered, moving the crack velocity line in the velocity–pressure diagram. The equilibrium velocity would be changed or the intersection between the curves could be lost, in which case the crack would arrest.

The axial bending strain for all the gas pipeline tests is about 0.5%–1% for stable propagation conditions. This is well below the ductilities expected of pipeline materials and so the model is consistent with the observed absence of multiple cracking. The azimuthal bending strains are smaller. Typical radial displacements lie in the range 1.5–3 cm for these tests, corresponding to crack openings of about 9–18 cm or about 0.4 radii. Often much larger displacements have been seen which may indicate a deficiency in the modelling. However, the success in accounting for propagation conditions is encouraging enough to apply the model to reactor situations.

4. Reactor coolant pipe rupture

In this section we apply the rupture model to the case of the rupture of PWR hot leg pipes. The geometry and operating conditions of a typical PWR hot leg pipe were described recently (Bhandari, 1993). The main difference is that the pressurized fluid is steam, with $\gamma \approx 1.33$ and a high velocity of sound at 343 °C of 613 m s^{-1}. The geometry and some of the physical properties are shown in Fig. 6; in addition, we take the Young's modulus to be 172 GPa, the initial pressure to be 15.5 MPa and the wall density to be 8000 kg m^{-3} (Bhandari, 1993). The decompression curve lies

above the crack velocity or energy balance curve, which suggests that a crack will not propagate in equilibrium for such a situation. The yield stress and toughness assumed may be low estimates (Bhandari, 1993), but increasing them will only reduce the crack velocity curve further and reinforce our conclusions. The main reason for the absence of steady state propagation is that the steam depressurizes very rapidly.

Experimental measurements of the velocity of cracks in pipes of various geometries were also reported in Bhandari and Leroux (1993). The tests were conducted in the early 1980s at CEA Cadarache and MPA Stuttgart. A summary of the calculations is given in Table 2. In the CEA tests, pipes of outer diameter 88.9 mm and thickness 3.09 mm were used and the tests were conducted at 235 °C. Unfortunately, it was stated only that the pipes were made from a stainless steel; other experimental details were missing. Following the PWR hot leg example, of which the tests described in Bhandari and Leroux (1993) are meant to be representative, we assume an initial pressure of 15.5 MPa, a yield stress of 174 MPa, a Young's modulus of 172 GPs, a density of 8000 kg m^{-3} and a toughness of 131 MPa m$^{1/2}$, together with $\gamma = 1.4$ (for a pressurizing medium of air) (Bhandari, 1993); a decompression curve and a crack velocity curve can be generated similar to those shown in earlier figures. Stable propagation is

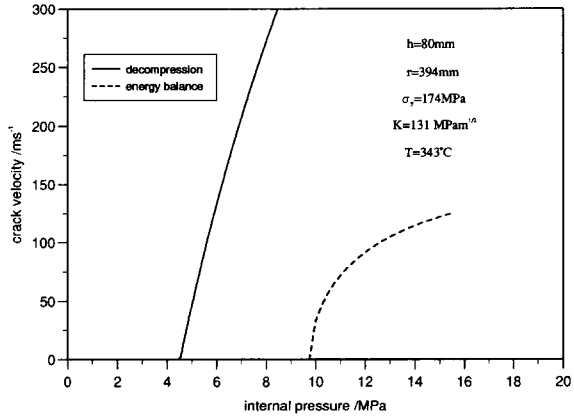

Fig. 6. Energy balance and decompression curves for typical PWR hot leg pipework geometry (Bhandari, 1993), suggesting that steady propagation is not supported.

Table 2
Parameters and comparison between predicted and measured crack propagation velocities for pipe rupture tests reported in Bhandari and Leroux (1993)

	Cadarache	Stuttgart
r (mm)	44.45	400
h (mm)	3.09	47.5
ρ_c (kg m^{-3})	8000	8000
T (°C)	235	245
σ_y (MPa)	174	174
E (GPa)	172	172
γ	1.4	1.4
p_L (MPa)	15.5	15.5
K (MPa m$^{1/2}$)	131	131
v_{calc} (m s^{-1})	140	None
v_{expt} (m s^{-1})	96	40–95

predicted at about 140 m s^{-1}. The mean velocity observed in three tests was 96 m s^{-1} (Bhandari, 1993). By assuming slightly different values of the yield stress for the pipe material, bearing in mind that the experimental conditions are uncertain, theory and experiment might be brought into better agreement.

In the Stuttgart tests we have $r = 400$ mm and $h = 47.5$ mm. Here the material was said to be a ferritic steel, but its properties were not specified (Bhandari, 1993). Assuming the other parameters are the same as in the CEA tests and with $T = 245$ °C, the model predicts that there is no stable crack propagation state, although by adjusting the material properties, which might be allowable considering the uncertainty in the reported experiments, such a stable state might well be identified with a velocity within the observed range of 40–95 m s^{-1} (Bhandari, 1993).

Clearly, without full information about the materials and the test conditions, no satisfactory test of the crack propagation model can be made. The rough calculations given here, however, suggest that predictions of the correct order of magnitude are being made.

5. Fuel pin rip propagation

The missing element of a complete model of crack propagation in ruptured fuel pins is a de-

scription of pin depressurization. Unless the fuel–clad gap is open at failure, in which case the pin is effectively gas pressurized, the previous model cannot be used. Preliminary calculations of relaxation of a compressed solid bar, on releasing the load at one end, do not yield an equivalent description of a finite crack tip pressure as in Eq. (13), but rather predict a step-like decompression front which moves away from the fracture at the speed of sound in the bar. In the absence of a complete model, however, predictions can still be made. Fig. 7 shows the results of crack velocity calculations with $\alpha = 14$ for a tube typical of fuel pin cladding with $r = 4$ mm, $h = 0.5$ mm, $\sigma_y = 300$ MPa and $K = 100$ MPa m$^{1/2}$. The yield pressure was 37.5 MPa. Over the range of possible driving pressures the crack velocity ranges from zero to about 225 m s^{-1}, with a minimum driving pressure of about 12 MPa or $0.32p_y$. The actual driving pressure will depend on the initial pressure and the decompression mechanism. If the pressurizing medium were a high temperature gas with a higher speed of sound than in the case of the low temperature gas pipe tests, then the decompression curve would intersect the crack velocity curve in the 12–15 MPa driving pressure range, with $v \approx 100$ m s^{-1}.

Fig. 7 also shows the axial bending strain ϵ_z over the possible range of pressure. Where v is non-zero, ϵ_z ranges between about 4% and 14%. For the gas depressurization case referred to above, ϵ_z would lie between 4% and 7%. Whether

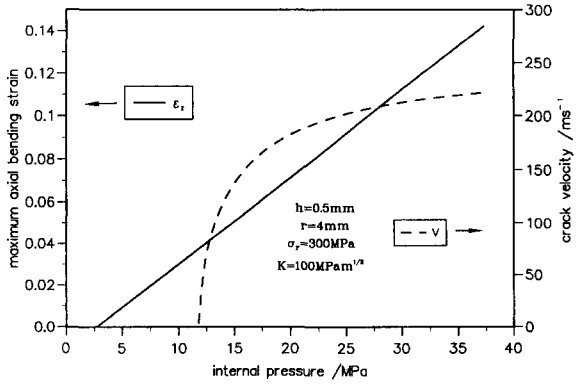

Fig. 7. Axial bending strain and crack velocity against internal pressure for fuel pin geometry.

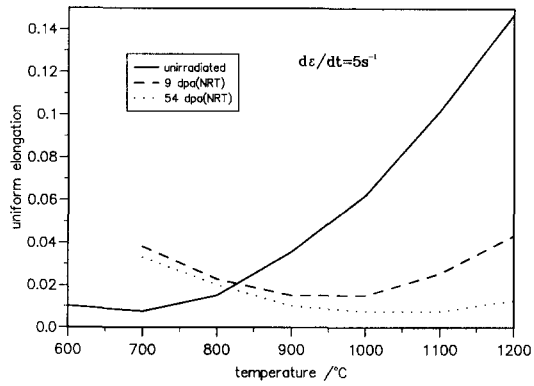

Fig. 8. Dependence of uniform elongation of 20% CW AISI 316 steel on test temperature and irradiation history.

the tube fragments then depends on the available ductility of the material. This is affected by the temperature, strain rate and irradiation history, so predictions depend on the precise conditions at failure. 20% cold-worked (CW) AISI 316 stainless steel has been a benchmark fast reactor fuel pin cladding material for many years and its properties are well established. Fig. 8 reproduces CABRI-1 data reported in Balourdet and Cauvin (1990) on the uniform elongation (UE) of this material at a high strain rate of 5 s^{-1} and over a range of temperatures. A reduction in UE is apparent after irradiation. Pins with the dimensions and properties given above and fractured, for example, at 1000 °C would therefore be likely to fail with a single crack geometry before irradiation, but would fragment if tested after irradiation. The crack length at the onset of fragmentation would be about $2a$ or $2(14rh)^{1/2}$, which is about 10.6 mm for the given geometry or just over one diameter of the pin.

The revised crack propagation model has been included within the TRAFIC fuel pin modelling code (Matthews, 1986) and used in the analysis of a selection of pin failure tests in the CABRI-1 programme (Cranga, 1990). These involve subjecting a fuel pin to an overpower transient such that the cladding tube suffers high strains. The pin cladding material was 20% CW AISI 316. The results are given in Table 3. A range of ϵ_z can be deduced corresponding to possible crack velocities between zero and the maximum velocity shown,

as in Fig. 7. The temperature of the test allows comparison of ϵ_z with the clad ductility: test A3 used a fresh pin and the others involved pins irradiated to 9 dpa(NRT). The CABRI-1 programme included many other tests, some on pins irradiated to 60 dpa(NRT), but this sample set will serve as an illustration of the model. In all cases the minimum axial bending strain exceeds the uniform elongation and so multiple cracking would seem to be favoured. It is not easy to distinguish experimentally between single and multiple cracking, however, owing to the destruction of the pin later in the transient, but initial measurements indicate an axial extent of the pin rupture of about 2 cm (Cranga, 1990), similar to the estimated length suggested above at which arrest by fragmentation occurs.

6. Discussion and conclusions

The model of axial crack propagation in ruptured tubes developed here is based on the mechanics of crack geometry and energy flows. Using a model of gas decompression at the tip of a running crack, a description of the propagation of a rupture in gas pipes of 1 m diameter has been developed which has a number of desirable features. Firstly, it can account for the propagation velocities of cracks in a number of gas pipeline tests. Secondly, a minimum initial pressure for steady propagation emerges, consistent with the threshold suggested by Maxey et al. (1973, 1974). Thirdly, the propagation conditions are stable against small perturbations. In this respect the model is more satisfactory than that developed by Freund and Parks (1980). The model has been applied to the interpretation of fuel pin rupture tests in the CABRI-1 programme (Cranga, 1990).

Table 3
Calculations of axial bending strains ϵ_z and upper limits on crack velocities v for tests in the CABRI-1 series (Cranga, 1990), assuming $\sigma_0 = \sigma_y$

	A3	BI2	AI3	BI4
σ_0 (MPa)	278	255	543	275
T (°C)	720	896	685	1129
ϵ_z (%)	4–15	3.5–14	3.4–16	3.5–15
v (m s^{-1})	212	205	300	212

The model developed here from earlier work (Ford, 1992a) contains a criterion for the appearance of multiple cracks. This is encountered when axial bending strains greater than the ductility are produced in the flaps behind the crack tip. Strains are low (about 1%) for the gas pipeline tests but relatively high (up to 15%) in calculations of fuel pin rupture. This reflects a proportionality between ϵ_z and h/r, which follows from Eqs. (1), (11) and (14). Multiple cracking therefore appears likely in fuel pin cases, especially after irradiation when ductilities are low (Fig. 8) (Balourdet, 1990). This would limit the axial extension of a pin rupture but increase the area of fracture compared with the single-crack mode. However, experimental support for this criterion is lacking at present.

Further work would be necessary in order to refine the model and examine the sensitivity of the fragmentation criterion to uncertainties in the mechanics discussed earlier. The form taken by the deformation is assumed and parametrized by radial displacement δ and axial extent a. A function relation between the two is found by an approximate mechanical analysis and the other is fitted to data. The tube is treated as a thin shell and the wall material is taken to be rigid–perfectly plastic. Future development ought to improve the mechanical analysis, taking into account stress biaxiality and combined bending and tension as well as a realistic axial profile of driving pressure. Some allowance for elastic bending and work hardening should be made. For fuel pins the decompression of molten fuel should be considered in greater depth than hitherto (Ford, 1992a). Data on the rupture of gas-pressurized fuel pins would be extremely useful. Nevertheless, the model seems to describe the data quite well and probably contains the essence of the physics involved.

Acknowledgement

This work was performed as part of the Fast Reactor Safety Programme of AEA Technology,

funded by the UK Department of Trade and Industry.

References

M. Balourdet and R. Cauvin, Transient mechanical properties of CABRI-1 cladding (CW 316), Proc. BNES Conf. on Fast Reactor Core and Fuel Structural Behaviour, Inverness, 1990.

S. Bhandari and J.C. Leroux, Evaluation of crack opening times and leakage areas for longitudinal cracks in a pressurized pipe. Part II. Application of proposed model and fracture dynamics, Nucl. Eng. Des. 142 (1993) 21.

D. Brock, Elementary Engineering Fracture Mechanics, Sijthoff and Noordhoff, 1978, Chap. 9.

K. Buxton, G.W. Pemberton and G.A.B. Linekar, unpublished work.

M. Cranga, D. Struwe, W. Pfrang, D.J. Brear and N. Nonaka, Transient material behaviour in CABRI-1 experiment failure under fully and semi-restrained fuel pin conditions, Proc. Int. Fast Reactor Safety Meet., Snowbird, UT, 1990, Vol. 1, p. 421.

I.J. Ford, Axial crack propagation in fuel pin cladding tubes, Nucl. Eng. Des. 136 (1992a) 243.

I.J. Ford, Rupture of pressurised tubes by multiple cracking and fragmentation, AEA-InTec-0829, 1992b; Int. J. Press. Vess. Piping 57 (1994) 21.

I.J. Ford, Axial cracking of cladding tubes loaded by solid fuel pellets, Harwell Rep. AEA-InTec-0782, 1992c.

L.B. Freund and D.M. Parks, Analytical interpretation of running ductile fracture experiments in gas-pressurised linepipe, ASTM STP 711 (1980) 359.

G.T. Hahn, M. Sarrate, M.F. Kanninen and A.R. Rosenfield, Int. J. Fract. 9 (1973) 209.

K.D. Ives, A.K. Shoemaker and R.F. McCartney, J. Eng. Mater. Technol. 96 (1974) 309.

M.F. Kanninen, S.G. Sampath and C. Popelar, J. Press. Vess. Technol. 98 (1976) 56.

H.W. Liepmann and A. Roshko, Elements of Gasdynamics, Wiley, New York, 1957, p. 62.

J.R. Matthews, R.F. Cameron, P.E. Coleman and R. Thetford, The application of the TRAFIC code to fast reactor fuel transients, Proc. BNES Conf. on Fast Reactor Safety, Guernsey, May 1986.

W.A. Maxey, J.F. Kiefner, R.J. Eiber and A.R. Duffy, Proc. 12th World Gas Conf., International Gas Union, Nice, 1973.

W.A. Maxey, R.J. Podlasek, R.J. Eiber and A.R. Duffy, Observations on shear fracture behaviour, British Gas/IGE Symp. on Crack Propagation in Pipelines, Newcastle, March 1974.